

# Compensation of RF-Induced Energy Spread in the CEBAF Injector Chopping System\*

M. G. Tiefenback and G. A. Krafft,  
Continuous Electron Beam Accelerator Facility,  
12000 Jefferson Avenue, Newport News, VA 23606-1909 USA

## Abstract

The CEBAF injector chopping system must generate three interleaved 499 MHz pulse trains of independently variable current from a DC input beam prior to axial compression. The chopper consists of two deflection cavities with an aperture midway between them. Lenses flanking the aperture focus the beam from the first cavity into the center of the second, where the RF deflection from the first cavity is removed. The symmetry of the RF energy spread across any time-slice of the beam is dominantly odd. The inverting optics used to focus the beam into the second cavity causes near cancellation of the energy spread from the two cavities. We present experimental measurements of the energy spread effects from a fundamental frequency (1497 MHz) chopper prototype producing a beam of suitable transverse emittance and energy spread, and discuss the expected performance of the subharmonic chopper system to be used for commissioning starting in January, 1994.

## I. INTRODUCTION

The present CEBAF chopper design [1] follows closely the design of the chopper for the NBS microtron [2], and consists of two circularly polarized  $TM_{210}$  deflection cavities, an aperture plate, and a pair of solenoid lenses, as shown in Fig. 1. The first cavity (C1) steers the incom-

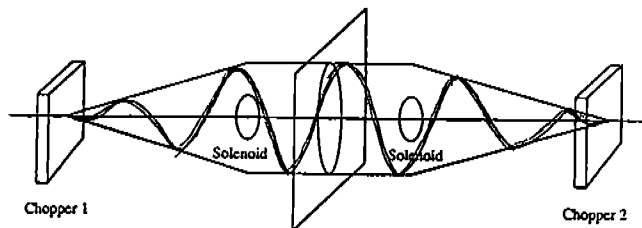


Figure 1. Sketch of the CEBAF injector beam chopping system.

ing DC beam along a divergent cone toward the chopping aperture plate. The first lens directs the beam parallel to the beamline. The second lens directs the beam along a

convergent cone with a focus at the center of the second cavity (C2). Cavities C1 and C2 must provide identical deflections to each slice of the beam in order for the overall deflection to be zero. In the absence of an aperture plate, the entire beam is closely restored to its DC state. The beam outline is helical between the cavities, although each electron follows a path at constant azimuth with respect to the beamline.

For like circular polarizations in the two cavities, multiple equivalent apertures may be placed on the aperture plate. Chopping system operation at the third subharmonic of the fundamental linac frequency with three variable apertures  $120^\circ$  apart on the aperture plate will provide three 499 MHz pulse trains with independently controllable current.

## II. SINGLE CAVITY EFFECT

The CEBAF deflecting cavities are square, with inner dimensions of 22.39 cm transverse to and 4.0 cm along the beamline. The mode structure of the vertically deflecting linearly polarized  $TM_{120}$  mode is (adapted from [3])

$$E_{vz} = -\sqrt{5}\eta H_0 \cos \frac{\pi x}{a} \sin \frac{2\pi y}{a} \sin \omega t \quad (1)$$

$$H_{vz} = -H_0 \sin \frac{\pi x}{a} \sin \frac{2\pi y}{a} \cos \omega t \quad (2)$$

$$H_{vx} = -2H_0 \cos \frac{\pi x}{a} \cos \frac{2\pi y}{a} \cos \omega t, \quad (3)$$

in mks units, plus the corresponding expressions for the orthogonal mode. Here  $a$  is the transverse dimension of the cavity,  $\omega$  is the angular frequency of the RF,  $\eta = \sqrt{\epsilon_0 \mu_0}$ , the origin is the center of the cavity,  $x$  is positive to the left and  $y$  is positive upward with respect to the beam, and  $z$  is in the direction of motion of the beam. Fig. 2 illustrates a beam being deflected upward in a left circularly polarized system. The upward deflection is followed by deflection to the left, implying a positive value of  $H_y$  for electrons. For maximal vertical deflection, the particles cross the center of the cavity at time  $t = 0$ , corresponding to zero crossing for  $E_{vz}$ .

We will neglect the field distortion at the entrance and exit apertures. For the beam energy of 100 keV, the beam samples RF phases approximately over  $\pm 1.2$  rad over the 4 cm length of the cavity. The momentum  $\delta p_y$  imparted to the particles from the vertically deflecting mode in the

\*This work was supported by the U.S. Department of Energy, under contracts No. #DE-AC05-84ER40150.

cavity is

$$\delta p_y = \frac{q_e v_z}{\omega} \int_{-1.2}^{1.2} \mu_0 H_{vx}(\psi) d\psi \quad (4)$$

where  $q_e$  is the charge and  $v_z$  is the velocity of the electron. The longitudinal momentum at this kinetic energy is 335 keV/c and the deflection angle is approximately 10 mrad. The maximum magnetic deflecting field  $2\mu_0 H_0$  is then approximately 3.5 G and the maximum gradient in the electric field is  $E'_z = 3.3$  MV/m<sup>2</sup>.

For the horizontally deflecting mode in a left circularly polarized system,

$$E_{hz} = \sqrt{5}\eta H_0 \cos \frac{\pi y}{a} \sin \frac{2\pi x}{a} \cos \omega t. \quad (5)$$

Approximations for small deviations off-axis for Eqs. 1 and 5 are

$$E_{vz} = -\frac{2\pi\sqrt{5}}{a}\eta H_0 y \sin \omega t \quad (6)$$

and

$$E_{hz} = \frac{2\pi\sqrt{5}}{a}\eta H_0 x \cos \omega t. \quad (7)$$

The energy integral for  $E_{vz}$  (an odd function over a symmetric interval) is zero along a line parallel to the  $z$  axis, so a constant offset does not affect the energy gain of a particle. To first order in  $x$  and  $y$ , all particles leave the cavity with the same energy increment from  $E_{vz}$ . Approximating the deflection as a uniform force resulting in a deflection  $\delta\theta$  over a path of length  $L$ , the energy change is approximately

$$q_e E'_z \frac{\delta\theta}{2L} \left(\frac{v_z}{\omega}\right)^3 \int_{-1.2}^{1.2} (\psi + 1.2)^2 \sin \psi d\psi.$$

Only the term linear in  $\psi$  survives, and for our parameters  $\Delta E$  is +4.8 eV. The electric field for the other RF mode, however, is at its maximum during the particle crossing, and the energy change neglecting the slight  $x$  deflection is

$$\frac{q_e v_z x}{\omega} E'_z \int_{-1.2}^{1.2} \cos \psi d\psi,$$

for a total energy change of 105 eV per millimeter of horizontal offset from the center of the cavity for particles being

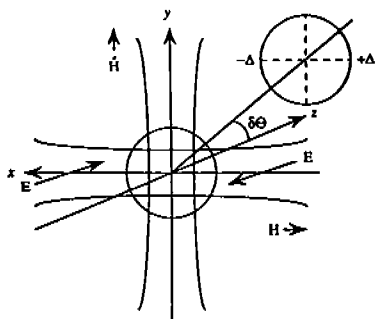


Figure 2. Left circularly polarized deflection cavity, beam deflected upward.

deflected vertically. This pattern rotates in time, so that at any point along the subsequent path of the beam, the particle energies are the same along any radius from the original beamline, but there is a gradient in the azimuthal direction. These analytic results are in good agreement with particle simulations by Liu, *et al.* [4]. This correlation of energy with position is used to search for the RF energy spread, as described below.

The beam passes through an emittance filter just before entering the first cavity, limiting the radius of the beam to less than 1.85 mm in the cavity. The resulting  $\pm 190$  eV spread in energy would degrade the final bunching process, especially if increased by passage through the second cavity. The rms energy spread introduced by a single cavity (90 eV), corresponds to an rms momentum spread of  $5 \times 10^{-4}$ . The energy spread from the DC high voltage supply for the gun is less than  $10^{-4}$ , so the relative momentum spread should be less than  $6 \times 10^{-5}$  with no RF on.

### III. MEASUREMENT RESULTS

We steered the beam through the chopper system with the RF off and measured the beam diameter at a spectrometer with a horizontal dispersion of 43 cm, using a scanning wire monitor (profile A in Table 1). We repeated this with RF on in C1, using steering magnets to deflect the outgoing beam cone so that first the top portion (profile B) and later the bottom portion (profile C) of the cone passed across the central aperture on the plate. The profiles for these two beam setups are shown in Fig. 3.

With both choppers on, profile D was taken with beam passing through a 60° slot at the top of the circle and profile E was taken with beam passing through a 60° slit at the bottom of the circle. These profiles are narrower than profile A with the choppers off, which may indicate the presence of an instrumental artifact, a current-dependent increase in the measured profile. With the RF on, the central hole passes 11.5° (FWHM) of the RF cycle, so thirty times as much current reaches the profile monitor with the RF off (profile A) as for profiles B and C. Profiles D and E were taken using a 60° slit, and have an intermediate current. Profiles B and C (Fig. 3) are for equal beam currents, as are profiles D and E. The rms beam radii were 0.61 mm and 1.28 mm with one cavity on, and 0.48 mm and 0.56 mm with both cavities on.

Table 1. Variances of beam profiles

label	RF status	$x_{rms}$ (mm)	$\delta\theta_y$ (radian)
A	off	0.63	0
B	C1 on	0.61	+0.01
C	C1 on	1.28	-0.01
D	C1,C2 on	0.48	+0.01
E	C1,C2 on	0.56	-0.01

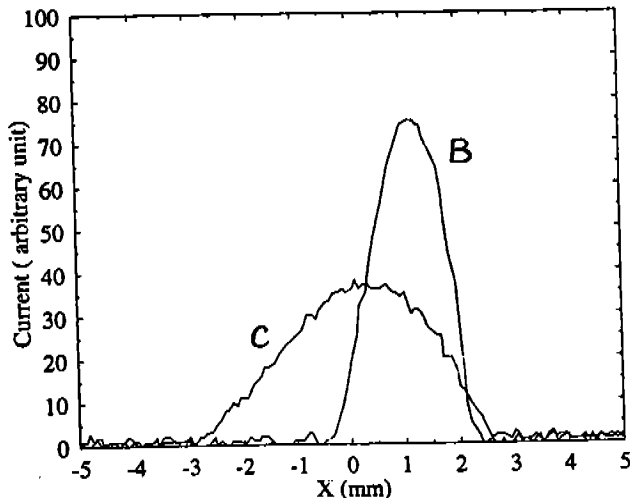


Figure 3. Profiles of the 100 keV beam in a region of horizontal dispersion 43 cm. See text for discussion.

#### IV. ANALYSIS

The profile asymmetry is due to the  $\langle x\delta p_z \rangle$  and  $\langle x'\delta p_z \rangle$  correlations introduced by the RF cavities. If the energy spread were uncorrelated with the horizontal coordinate of the beam, there would be no difference between beam from the top of the circle and beam from the bottom. The correlation  $\sigma_{11} = \langle x^2 \rangle$  at the profile monitor is related to the correlation matrix at the second chopper cavity by

$$\sigma_{11} = M_{1k} \Sigma_{kl} M_{l1},$$

where  $M_{ij}$  is the transfer matrix between the two points and  $\Sigma_{kl}$  is the correlation matrix at the cavity. Samples of the beam taken at the top and bottom of the chopper circle will differ only in the sign of  $\langle x\delta p_z \rangle$  (and the consequent  $\langle x'\delta p_z \rangle$ ). Therefore the mean square difference between the downstream profiles for these portions of the beam will be proportional to the momentum correlation terms.

From Table 1, the difference in mean square (not rms) radius between profiles B and C is  $12.7 \times 10^{-7} \text{ m}^2$  while the difference between D and E is only  $0.8 \times 10^{-7} \text{ m}^2$ . Profiles D and E are both smaller than profiles B and C, in spite of the factor of six higher current and even higher relative current density. This indicates a cancellation of the correlated energy spread introduced by a single cavity by approximately a factor of fifteen.

There are some points of disagreement concerning the actual energy spread of the beam with and without the RF cancellation. The overall rms width of profile B plus profile C is 1 mm, which is the profile width that would be measured from summing the two beam distributions at the chopper cavity to remove the correlated energy spread without changing the rms momentum spread. To account for the increase in rms radius with respect to A, D, and E purely through increased energy spread would require an energy spread for a single cavity of  $2 \times 10^{-3}$ , which is more than three times the calculated value. The RF-induced emittance increase from using a single deflection

cavity (limited by the central  $11.5^\circ$  aperture as a stop in the system) should be well under a factor of two, and at this level cannot reconcile the observation and calculation.

#### V. CONCLUSIONS

A large difference in the measured beam size results from changing the sign of the RF  $\langle x\delta p_z \rangle$  correlation for a single cavity. The difference between the mean squares of profiles D and E with both deflection cavities powered (0.29 mm) is smaller by a factor of fifteen than that of B and C (1.13 mm) with one cavity powered. This indicates more than an order of magnitude cancellation for the correlated energy spread induced by one cavity. For either sign of this correlation with both cavities on, the measured beam size is smaller than either of the one-cavity profiles and for the DC beam profile with no RF. In spite of possible instrumental problems, this supports the conclusion that the overall energy spread induced by the chopper system is significantly smaller than the effect of one cavity. The rms momentum spread induced by a single cavity seems to be significantly larger than expected from RF calculations and from the modeling results reported in [4].

Aberrations in the lenses and in the deflecting cavities remain as sources of increased emittance, and energy perturbations of even symmetry are not compensated. The time-of-flight error between the cavities caused by the energy modulation is negligible. Any deviation from unity for the optics magnification from C1 to C2 will result in reduced cancellation of the energy spread.

The subharmonic chopper to be used at CEBAF is scaled from the fundamental frequency system, with one-third of the frequency and three times the deflection angle. The energy spread induced by the RF scales as  $\omega\delta\theta$ , and should be unchanged from the 1497 MHz system. There is a greater spacing planned between the cavities, but the phase lag from the differential velocity of the particles between the cavities is still unimportant.

#### VI. REFERENCES

- [1] W. Diamond and R. Pico, 1988 Linac Conf., CEBAF-Report-89-001, June, 1989, pp. 403-405.
- [2] M. A. D. Wilson, *et al.*, "Performance of the 100 keV Chopper/Buncher System of the NBS-Los Alamos RTM Injector," Proc. 1985 Part. Acc. Conf., IEEE Trans. on Nuc. Sci., NS-32 (5), pp. 3089-3091.
- [3] Jacob Haimson, "Optimization Criteria for Standing Wave Transverse Magnetic Deflection Cavities," Proc. of the 1966 Linear Acc. Conf., Los Alamos Scientific Laboratory, LA-3609, pp. 303-331.
- [4] H. Liu and J. Bisognano, "Simultaneous Cancellation of Beam Emittance and Energy Spread in the CEBAF Nuclear Physics Chopping System," these proceedings.